Chemical Geology 386 (2014) 209–217

Contents lists available at ScienceDirect

Chemical Geology

journal homepage: www.elsevier.com/locate/chemgeo

Production of branched tetraether lipids in Tibetan hot springs: A possible linkage to nitrite reduction by thermotolerant or thermophilic bacteria?☆

Fuyan Li [a], Chuanlun L. Zhang [a,b,*], Shang Wang [c], Yufei Chen [a], Chijun Sun [a,d], Hailiang Dong [c,e], Wenjun Li [f], Martin G. Klotz [g], Brian P. Hedlund [h]

[a] State Key Laboratory of Marine Geology, Tongji University, Shanghai 200092, China
[b] Department of Marine Sciences, University of Georgia, Athens, GA 30602, United States
[c] State Key Laboratory of Biogeology and Environmental Geology, China University of Geosciences, Beijing 100083, China
[d] Department of Earth and Planetary Sciences, Northwestern University, Evanston, IL 60208, United States
[e] Department of Geology and Environmental Earth Science, Miami University, Oxford, OH 45056, United States
[f] Yunnan Institute of Microbiology, Yunnan University, Kunming 650091, China
[g] Department of Biological Sciences, University of North Carolina, Charlotte, NC 28223, United States
[h] School of Life Science, University of Nevada Las Vegas, Las Vegas, NV 89154, United States

ARTICLE INFO

Article history:
Received 18 April 2014
Received in revised form 7 August 2014
Accepted 8 August 2014
Available online 17 August 2014

Editor: J. Fein

Keywords:
Branched glycerol dialkyl glycerol tetraethers
Hot springs
Tibet
Nitrite reduction

ABSTRACT

Branched glycerol dialkyl glycerol tetraethers (bGDGTs) are produced by bacteria and originally identified from soils and peat bogs; recently, however, in situ production of bGDGTs in hot springs has been reported. Consequently, we designed this study to evaluate the linkage between the distribution of bGDGTs, their biological sources and inferred metabolic processes based on the distribution and abundance of bGDGTs, pertinent water chemistry, the *nirS* gene (possibly in *Beta-* and *Gamma-proteobacteria*) and available 16S rRNA (tag) gene pyrosequencing data from 37 Tibetan hot springs. The absolute and relative concentrations of intact polar and core bGDGTs suggest that bGDGTs are predominantly produced in situ in these hot springs. Redundancy analyses revealed correlations between the distribution of bGDGTs and concentrations of ammonium, nitrite, and nitrate and the abundance of *nirS* gene, which are better reflected in the core bGDGT fraction than in the respective intact polar bGDGT fraction. Reanalysis of published bacterial 16S rRNA gene sequences showed that residence of members of the bacterial phyla *Proteobacteria* and *Bacteroidetes* correlated positively with a new methylation index ($R_{(III + II)/I}$) of bGDGTs. Some representatives of these taxa examined in this study are capable of *nirS*-encoded nitrite reduction, suggesting that bGDGT-synthesizing bacteria might be affiliated with these two phyla in Tibetan hot springs.

1. Introduction

Branched glycerol dialkyl glycerol tetraethers (bGDGTs; structures presented in Fig. 1) were discovered in samples from peat bogs and identified as a new group of cell membrane lipids (Sinninghe Damsté et al., 2000). The bGDGTs exhibit a mixture of archaeal (transmembrane tetraethers) and bacterial (branched alkyl chains) traits; nevertheless, the bGDGTs have 1,2-di-*O*-alkyl-*sn*-glycerol stereochemistry (Weijers et al. 2006a), which is diagnostic for lipids of bacteria (Wächtershäuser, 2003 and references therein).

The bGDGTs are ubiquitous in soils and peat deposits (Sinninghe Damsté et al., 2000; Schouten et al., 2000; Weijers et al., 2006a, 2006b; Peterse et al., 2009a, 2010, 2012; Liu et al., 2010) and have also been identified in lakes (e.g. Powers et al., 2004; Blaga et al., 2009), coastal marine sediments (Schouten et al., 2000; Hopmans et al., 2004) and hot springs (e.g. Schouten et al., 2007; He et al., 2012; Hedlund et al., 2013; Zhang et al., 2013). In an empirical study of about 130 soils worldwide, Weijers et al. (2007a) found significant linear correlations between bGDGT compositions and annual mean air temperature (MAT) or soil pH, which are expressed by two novel indices, the Methylation of Brached Tetraethers (MBT) index and the Cyclisation of Branched Tetraethers (CBT) index. The MBT and CBT indices have been successfully applied to reconstruct past continental temperatures and soil pHs (Weijers et al., 2007b, 2007c, 2011; Ballantyne et al., 2010; Bendle et al., 2010; Fawcett et al., 2011; Peterse et al., 2011b; Rueda et al., 2009; Schouten et al., 2008; Tyler et al., 2010; Zhou et al.,

☆ This work was conducted in the State Key Laboratory of Marine Geology at Tongji University.

* Corresponding author at: State Key Laboratory of Marine Geology, Tongji University, Shanghai 200092, China. Tel.: +86 2165982012; fax: +86 2165988808.
E-mail address: archaea.zhang@gmail.com (C.L. Zhang).

http://dx.doi.org/10.1016/j.chemgeo.2014.08.015
0009-2541/

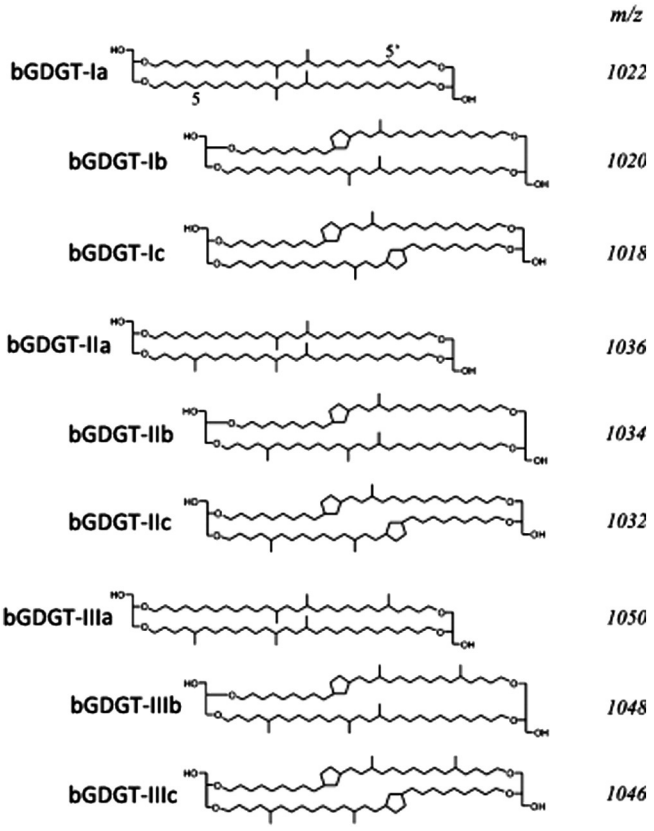

Fig. 1. The structures of bacterial core lipids examined in Tibetan hot springs.

2011; Zink et al., 2010). The bGDGTs recovered from aquatic systems in earlier studies were inferred to be attributed to contamination by erosion of the catchment soils; however, recent studies demonstrated that bGDGTs can be synthesized in situ in aquatic environments such as lakes (Sinninghe Damsté et al., 2009; Tierney and Russell, 2009; Sun et al., 2011; Tierney et al., 2011; Wang et al., 2012), fjords (Peterse et al., 2009b), estuaries (Zhu et al., 2011; Zhang et al., 2012) and hot springs (He et al., 2012; Hedlund et al., 2013; Zhang et al., 2013).

Upon cell death, intact polar lipids are degraded quickly into more recalcitrant core lipids by cleavage of the polar head groups; therefore, intact polar lipids were proposed to originate from living cells (Harvey et al., 1986; White et al., 1977). The head groups of intact polar (IP) bGDGTs have been identified to be sugars, phosphates, or a mixture of both (Liu et al., 2010; Peterse et al., 2011a). It has been recently suggested that the IP-bGDGTs may remain intact over a longer time than originally suspected (Liu et al., 2010; Schouten et al., 2010).

Although bGDGTs are widely distributed in nature, their source bacteria are still elusive. Weijers et al. (2009) combined organic geochemical- and diverse culture-independent techniques to propose *Acidobacteria* as potential biological sources of bGDGTs in peat bogs but failed to identify specific organisms. Examination of a suite of pure cultures of *Acidobacteria* identified only one bGDGT (bGDGT-I; Fig. 1) in the membranes of three aerobic strains (Sinninghe Damsté et al., 2011). However, abundant bGDGTs have been isolated from the anoxic layers of peat bogs (Weijers et al., 2006a; Peterse et al., 2011a), suggesting that other acidobacterial groups may contribute significantly to the detectable pool of bGDGTs. Recently, Zhang et al. (2013) reported a significant positive correlation between bGDGT abundance and the presence of certain thermophilic bacteria in a Great Basin hot spring, suggesting that bGDGTs in this hot spring may be produced in situ by thermophiles. Hedlund et al. (2013) expanded this study to other hot springs of the Great Basin and demonstrated that most bGDGTs are more abundant in hot springs than in surrounding desert soils, again suggesting that bGDGTs can be produced by thermophiles.

Here, we report the spatial distributions of core (C)- and IP-bGDGTs in Tibetan hot springs to evaluate an allochthonous or autochthonous origin of these lipids. We also examined the relationships between bGDGTs and environmental factors and attempted to link abundances of bGDGTs and the proteobacterial *nirS* gene (encoding the cytochrome cd1 nitrite reductase, Zumft, 1997 and Throbäck et al., 2004) in community DNA. Our data and the reanalysis of 16S rRNA gene pyrosequencing data published by Wang et al. (2013) implicate that the source organisms producing more bGDGTs with a high degree of methylation and less bGDGTs with a low degree of methylation in the studied hot springs may be bacteria affiliated with the phyla *Proteobacteria* and *Bacteroidetes*, some representatives of which have the capacity for *nirS*-encoded nitrite reduction as a major physiological trait.

2. Material and methods

2.1. Sampling

Thirty-seven surface sediment samples from hot springs and five surrounding surface soil samples were collected from Gulu (GL), Naqu (NQ), Guozu (GZ), Nima (NM) and Qucai (QC) regions on the Tibetan Plateau in the northwest of China (Fig. 2). The sampling locations, temperature and water chemical parameters were summarized in Table 1. Samples were frozen immediately in liquid nitrogen in the field and further stored at −80 °C in the lab. Temperature and water chemical parameters (i.e. pH, ammonium, nitrite and nitrate) in Table 1 have been reported in Li et al. (2013).

2.2. Lipid extraction and analysis

The total lipids were extracted using a sonication method and separated into apolar (alkane) and polar (C- and IP-bGDGTs) fractions following the procedure of Li et al. (2013). One aliquot of the polar fraction was directly screened by high-performance liquid chromatography-atmospheric pressure chemical ionization-mass spectrometry (HPLC-APCI-MS) (1200 Series/6460 Triple Quad, Agilent Technologies, Santa Clara, California, USA) when the other aliquot was acid hydrolyzed and subsequently analyzed on HPLC-APCI-MS. Conditions for HPLC-APCI-MS were set as stated in Li et al. (2013). The abundance of IP-bGDGTs was obtained using a subtraction method. Two samples, GL-S-1 and NM-2S, contained non-detectable C- and IP-bGDGTs but detectable archaeal tetraether lipids (Li et al., 2013).

The MBT and CBT calculations, based on the bGDGT distributions, were according to Weijers et al. (2007a):

$$\mathrm{MBT} = [\mathrm{Ia} + \mathrm{Ib} + \mathrm{Ic}]/[\mathrm{Ia} + \mathrm{Ib} + \mathrm{Ic} + \mathrm{IIa} + \mathrm{IIb} + \mathrm{IIc} + \mathrm{IIIa} + \mathrm{IIIb} + \mathrm{IIIc}] \quad (1)$$

$$\mathrm{CBT} = -\mathrm{LOG}([\mathrm{Ib} + \mathrm{IIb}]/[\mathrm{Ia} + \mathrm{IIa}]) \quad (2)$$

The Roman numerals in the equations referred to the bGDGT structures in Fig. 1.

2.3. Statistical analysis

Redundancy analysis (RDA) was performed using the software CANOCO for Windows version 4.5. The nine bGDGTs as response variables and environmental factors and log-transformed values of proteobacterial *nirS* gene copy numbers as explanatory variables were transferred into CANOCO software. Firstly, the lengths of the bGDGT composition gradients for four axes were measured by the detrended correspondence analysis (DCA) in the software CANOCO. As all of these lengths were shorter than 3 (data not shown), the RDA analysis based on a linear ordination method was suggested to be selected for

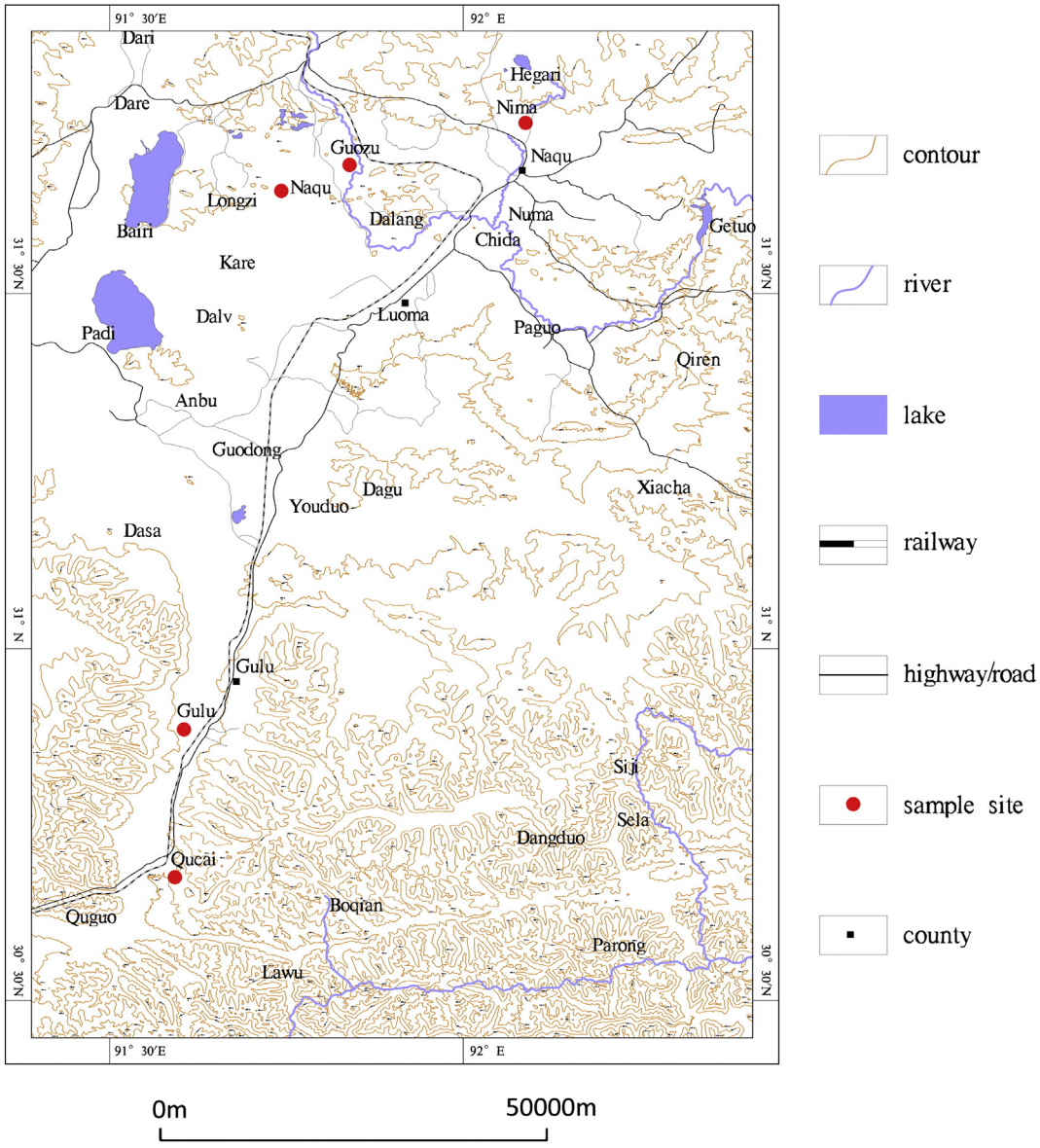

Fig. 2. A map of sampling locations of hot springs examined on the Tibetan Plateau, China. The geographic map was generated by software, Global Map and Google Earth.

our dataset (Jan Lepš and PetrŠmilauer, 2003). The variable significance was examined using Monte-Carlo significance test with permutation number of 999.

The correlations between bGDGTs and bacterial community from reanalysis of pyrosequencing data in some of the same hot springs were performed using SPSS software. These are GL-13-4, GL-20, GL-21, NQ-4, GZ-1, NM-6, NM-7, QC-2, QC-7 and QC-9, which have been analyzed using pyrosequencing method (Wang et al., 2013). We excluded the bacterial phyla that were present in no more than three samples. As a result, 15 bacterial phyla (*Acidobacteria*, *Aquificae*, *Armatimonadetes*, *Bacteroidetes*, *Chlorobi*, *Chloroflexi*, *Cyanobacteria*, *Deinococcus-Thermus*, *Firmicutes*, *Nitrospirae*, *Planctomycetes*, *Proteobacteria*, *Spirochaetes*, *Thermotogae* and *Verrucomicrobia*) were included in the following correlation analysis. These 15 bacterial phyla contributed more than 87% (usually 95%) to the bacterial community in each hot spring with the exception of QC-2, which had 26% contribution from these phyla. Thus the correlation analysis eventually included total nine hot spring samples (GL-13-4, GL-20, GL-21, NQ-4, GZ-1, NM-6, NM-7, QC-7 and QC-9) with both C- and IP-bGDGTs and 15 bacterial phyla and their affiliated genera.

3. Results

3.1. Temperature and water chemistry

Temperature of the Tibetan hot springs ranged from 22.1 °C to 80 °C, with the majority of springs being cooler than 75 °C (Table 1). The pH of the springs ranged between 7.0 and 9.1. The springs had relatively low concentrations of dissolved inorganic nitrogen (DIN, 6.5 to 42.5 μM; sum of NH_4^+, NO_2^- and NO_3^-), with individual species reaching 33.3 μM for NH_4^+, 16.8 μM for NO_2^-, and 17.7 μM for NO_3^- (Table 1). DIN pools in most springs were dominated by NH_4^+, with moderate concentrations of NO_2^- and low concentrations of NO_3^-. An exception was Nima (NM), in which NO_2^- and NO_3^- dominated (Table 1).

3.2. Absolute and relative abundances of bGDGTs

Both C- and IP-bGDGTs were detected in all of the hot springs and some of the surrounding soils. The total bGDGT concentrations ranged from 3.06 ng/g to 683.41 ng/g in the C-bGDGT fraction and from 0.53 ng/g to 111.53 ng/g in the IP-bGDGT fraction in all hot springs

Table 1
Information on the location, elevation (Elev.), temperature, water chemistry, absolute concentrations of total bGDGTs, MBT calculations for bacterial lipids, and bacterial *nirS* gene abundance from Tibetan hot springs (#1–37) and soil samples (#38–42). All data have been published in Li et al. (2013) except the bGDGT data.

		Location		Elev.	Temp.		NH_4^+	NO_2^-	NO_3^-	Total bGDGTs (ng/g)		MBT		CBT		*nirS*[g]
No.	Sample[a]	Lat. (N)[b]	Long. (E)[c]	(m)	(°C)	pH	uM	uM	uM	C-bGDGTs	IP-bGDGTs	C-bGDGTs	IP-bGDGTs	C-bGDGTs	IP-bGDGTs	(copies/g)
1	GL-4	30°52′14.9″	91°36′49.3″	4694	77.0	7.9	BD[f]	0.1	BD	11.64	1.42	0.58	0.69	0.39	1.08	1.94E + 08
2	GL-7	30°52′31.3″	91°36′42.9″	4702	66.0	8.8	5.0	0.1	0.2	108.63	4.98	0.81	0.55	0.66	0.93	2.36E + 10
3	GL-10	30°52′32.0″	91°36′38.8″	4708	80.0	8.8	2.2	BD	0.5	8.46	2.77	0.77	0.80	0.42	0.16	1.00E + 12
4	GL-13-3	30°52′33.0″	91°36′38.8″	4710	70.0	7.8	5.6	BD	1.3	3.22	0.85	0.44	0.24	0.32	0.80	1.10E + 10
5	GL-13-4	30°52′33.0″	91°36′38.8″	4710	66.0	7.8	5.6	BD	1.3	30.23	8.98	0.57	0.58	0.32	0.93	1.45E + 10
6	GL-13-5	30°52′33.0″	91°36′38.8″	4710	46.0	7.8	5.6	BD	1.3	36.97	10.43	0.62	0.58	0.50	0.72	1.85E + 11
7	GL-13-7	30°52′33.0″	91°36′38.8″	4710	56.0	7.8	5.6	BD	1.3	46.20	22.51	0.86	0.93	NA	0.71	4.54E + 10
8	GL-13-8	30°52′33.0″	91°36′38.8″	4710	42.0	7.6	5.6	BD	1.3	34.61	32.78	0.78	0.80	NA	0.27	7.98E + 10
9	GL-13-9	30°52′33.0″	91°36′38.8″	4710	27.0	7.6	5.6	BD	1.3	12.00	7.23	0.42	0.67	1.01	0.13	1.44E + 12
10	GL-15	30°52′34.1″	91°36′40.3″	4709	80.0	9.1	7.2	0.2	0.5	8.81	2.60	0.31	0.38	0.24	0.22	3.35E + 09
11	GL-16	30°52′34.8″	91°36′40.6″	4708	67.0	7.0	12.8	0.4	1.0	7.37	2.84	0.62	0.63	0.49	0.88	1.02E + 09
12	GL-20	30°52′34.9″	91°36′34.0″	4715	46.0	7.4	BD	0.9	ND	4.92	1.16	0.63	0.35	0.42	0.43	1.59E + 11
13	GL-21	30°52′34.9″	91°36′34.0″	4716	56.0	7.6	5.6	0.1	0.2	157.23	26.62	0.93	0.84	0.50	0.52	5.35E + 10
14	GL-22	30°52′34.3″	91°36′34.0″	4715	73.0	8.1	2.2	0.3	0.5	12.64	3.90	0.63	0.70	0.35	0.30	1.94E + 08
15	GL-24	30°52′42.9″	91°36′48.1″	4705	68.0	7.5	BD	BD	0.7	57.41	9.72	0.47	0.46	0.41	0.21	8.96E + 08
16	GL-26	30°52′43.6″	91°36′50.6″	4702	68.3	7.4	10.6	0.4	0.2	127.19	82.43	0.89	0.77	0.42	0.58	2.54E + 10
17	GL-30	ND[d]	ND	ND	49.0	7.3	1.7	BD	0.7	192.95	111.53	0.85	0.78	0.65	0.77	1.01E + 10
18	NQ-1	31°38′45.4″	91°45′8.0″	4555	54.0	7.4	28.9	11.5	1.6	49.33	1.41	0.39	0.52	0.10	0.34	2.44E + 11
19	NQ-2	31°38′45.6″	91°45′8.2″	4554	46.0	7.8	28.9	11.7	2.3	38.01	3.14	0.53	0.68	0.05	0.01	2.25E + 11
20	NQ-4	31°38′45.6″	91°45′8.2″	4554	48.0	7.8	33.3	10.7	1.3	12.40	1.39	0.36	0.50	0.39	0.58	1.93E + 11
21	NQ-5	31°38′45.1″	91°45′8.3″	4554	53.0	7.7	33.3	4.6	1.8	41.52	2.58	0.30	0.38	0.50	0.73	1.62E + 11
22	GZ-1	31°40′52.6″	91°51′21.4″	4610	22.1	7.2	3.9	5.7	2.7	314.38	90.13	0.26	0.29	0.32	0.49	1.66E + 12
23	GZ-2	31°40′54.1″	91°51′19.8″	4612	23.6	7.5	6.1	5.4	2.3	82.48	15.25	0.30	0.35	0.43	0.42	7.11E + 11
24	GZ-3	31°40′54.6″	91°51′18.9″	4612	21.9	7.5	18.9	6.3	2.4	31.89	3.62	0.40	0.65	0.41	0.27	6.38E + 11
25	NM-1	31°44′38.4″	92°5′59.2″	4642	50.0	7.3	6.1	13.2	17.7	10.97	0.85	0.33	0.08	0.20	0.30	1.66E + 12
26	NM-2	31°44′38.6″	92°5′59.6″	4642	51.0	7.0	0.6	15.4	15.5	3.06	0.53	0.58	0.68	0.42	0.77	2.52E + 13
27	NM-3	31°44′37.7″	92°5′56.2″	4639	42.0	7.0	1.7	15.7	15.5	31.71	8.22	0.25	0.29	0.27	0.43	1.28E + 13
28	NM-5	31°44′36.6″	92°5′55.2	4637	47.0	7.0	BD	15.3	4.0	40.04	9.57	0.52	0.58	0.40	0.41	3.08E + 12
29	NM-6	31°44′34.1″	92°5′57.4″	4635	48.0	7.0	BD	14.6	5.7	683.41	5.35	0.98	0.72	0.81	−0.18	1.94E + 11
30	NM-7	31°44′33.6″	92°6′0.9″	4636	43.0	7.0	BD	16.8	5.3	118.00	16.00	0.69	0.66	0.04	0.91	5.46E + 12
31	QC-1	30°40′0.4″	91°35′27.9″	4501	71.0	7.8	16.1	2.5	0.7	73.62	2.09	0.78	0.66	0.06	0.31	1.76E + 10
32	QC-2	30°52′0.2″	91°35′28.9″	4505	75.0	7.6	24.4	1.2	0.5	10.39	52.33	0.95	0.92	0.26	0.27	1.67E + 08
33	QC-4	30°39′59.2″	91°35′28.2″	4500	74.0	8.1	16.1	1.1	0.7	22.36	1.68	0.76	0.63	0.11	−0.03	4.26E + 09
34	QC-5	30°39′59.2″	91°35′28.2″	4500	74.0	8.0	10.0	0.9	0.2	14.70	0.57	0.76	0.77	0.14	−0.59	7.37E + 08
35	QC-7	30°39′58.6″	91°35′28.6″	4500	62.5	7.9	4.4	7.5	2.3	55.39	1.17	0.88	0.60	0.67	1.55	6.28E + 09
36	QC-8	30°39′57.7″	91°35′29.3″	4499	62.6	8.0	17.2	1.5	0.2	51.28	2.26	0.87	0.59	0.23	0.37	4.91E + 10
37	QC-9	30°39′58.0″	91°35′29.4″	4499	60.0	8.1	12.8	0.9	BD	49.07	3.49	0.84	0.74	0.21	0.29	2.77E + 11
38	GL-S-1	30°52′14.5″	91°36′49.7″	4714	ND	ND	ND	ND	ND	BD	BD	NA[e]	NA	NA	NA	ND
39	GL-S-2	30°52′14.3″	91°36′49.1″	4722	ND	ND	ND	ND	ND	7.55	0.36	0.36	0.30	0.08	−0.55	ND
40	NQ-S	31°38′45.4″	91°45′7.6″	4556	ND	ND	ND	ND	ND	6.96	0.48	0.87	0.58	0.74	0.69	ND
41	NM-2S	31°44′38.6″	92°5′59.6″	4642	ND	ND	ND	ND	ND	BD	BD	NA	NA	NA	NA	ND
42	QC-S	30°39′59.7″	91°35′29.8″	4507	ND	ND	ND	ND	ND	8.46	2.87	0.22	0.47	0.30	0.11	ND

[a] GL = Gulu region; NQ = Naqu region; GZ = Guozu region; NM = Nima region; QC = Qucai region; S = soil (GL-S-1 and GL-S-2 are sampled from Gulu region and close to the GL-4 hot spring. NQ-S locates above all the Naqu hot springs. NM-2S locates above all the Nima hot springs and near the NM-2 hot spring. QC-S locates above all the Qucai hot springs). See Fig. 1 for sample locations on the map.
[b] Latitude.
[c] Longitude.
[d] Not detected.
[e] Not available.
[f] Below detection.
[g] Originally, we did the RDA analysis on bGDGTs and environmental parameters and the results were similar to those described in the main text. As the most abundant bGDGTs were commonly found in the anoxic layers of peat bogs (Weijers et al., 2006a; Peterse et al., 2011a), the anaerobic metabolism was assumed to be the major process contributing to the production of bGDGTs. Because nitrogen species were correlated to bGDGTs, the *nirS* and *nirK* genes were selected to test the link between nitrogen-oxide transformation and the production of bGDGTs (the *nirK* gene experiment failed; data not shown). Bacterial *amoA* gene (targeting autotrophic ammonia-oxidizing bacteria) was not tested based on the understanding that all bGDGT producers are likely hetetrophic (Weijers et al., 2010).

examined (Table 1). Total C- and IP-bGDGTs were significantly correlated (Fig. 3a).

In the soil surrounding some of the hot springs, however, the total bGDGT concentrations ranged from below detection limit to 8.46 ng/g in the C-bGDGT fraction and from below detection limit to 2.87 ng/g in the IP-bGDGT fraction (Table 1), which were 1–2 orders of magnitude lower and showed less variation than in hot spring sediments. The C- and IP-bGDGTs in the surrounding soil samples were not significant correlated (Fig. 3b).

The MBT values calculated for hot spring bGDGTs ranged from 0.25 to 0.98 in the C-bGDGT fraction and from 0.08 to 0.93 in the IP-bGDGT fraction (Table 1). The MBT values for core and polar bGDGTs were significantly correlated (Fig. 3c).

3.3. Redundancy analysis (RDA)

RDA analysis was performed for C-bGDGTs and IP-bGDGTs to examine possible relationships between the compositions of bGDGTs and concentrations of environmental parameters and log-transformed values of proteobacterial *nirS* gene copy numbers (Table 1 and Fig. 4), which were published in Li et al. (2013). In the C-bGDGT fractions, the two axes explained 21% (14% for axis 1 and 7% for axis 2) of the bGDGT distribution and 80% (55% for axis 1 and 25% for axis 2) of the relations between bGDGTs and environmental factors and *nirS* gene abundance (Fig. 4a). The correlations between bGDGTs and environmental factors and *nirS* gene abundance were 0.581 on axis 1 and 0.648 on axis 2 (Fig. 4a). Since variables weighted much more

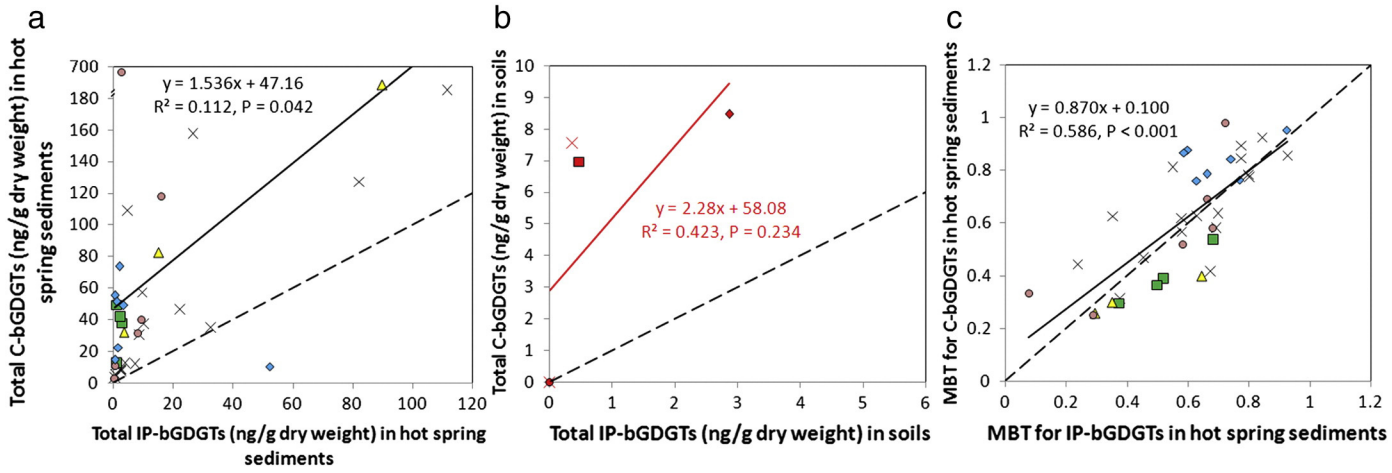

Fig. 3. Correlations between the core- and polar bGDGT fractions in absolute concentrations from hot spring sediments (a) and surrounding soils (b) and in MBT based on relative concentrations from hot spring sediments (c). The black lines with black equations show the linear correlation between C- and IP-bGDGTs from hot spring sediment samples (*R* square value and *P* value), whereas the red one represents the linear correlation from soil samples. The black dashed line represents the 1:1 line for each graph. X-marks represent hot spring sediment samples from Gulu region; green squares from Naqu region; yellow triangles from Guozu region; pink circles from Nima region; and blue diamonds from Qucai region (Table 1 and Fig. 2). The surrounding soil samples are labeled using red color with the same symbols as the counterpart hot spring sediment samples. For example, red X-mark represents soil sample from Gulu region, whereas black X-mark represents hot spring sediment samples from the same region. (For interpretation of the references to color in this figure legend, the reader is referred to the web version of this article.)

heavily on axis 1 than on axis 2, we focused on the explanation for axis 1 as follows. The bGDGTs with a high degree of methylation (i.e. bGDGTs-IIIa, -IIIb, -IIIc, -IIa, -IIb and -IIc; Weijers et al., 2007a) correlated positively with axis 1 whereas bGDGTs with low degree of methylation (i.e. bGDGTs-Ia, -Ib and -Ic) correlated negatively with axis 1 (Fig. 4a). Ammonium, nitrite, nitrate and *nirS* gene abundance varied positively with axis 1 whereas temperature and pH varied negatively with axis 1 (Fig. 4a). According to the lengths of vectors, temperature, ammonium, nitrite, nitrate and *nirS* gene abundance correlated strongly with bGDGT distribution whereas pH correlated weakly with bGDGT distribution (Fig. 4a). Temperature and pH correlated positively with less methylated bGDGTs (i.e. bGDGTs -Ia, Ib, Ic) and negatively with highly methylated bGDGTs (i.e. bGDGTs-IIIa, IIIb, IIIc, IIa, IIb, IIc). Ammonium, nitrite, nitrate and *nirS* gene abundance correlated positively with bGDGTs-IIIa, -IIIb, -IIIc, -IIa, -IIb and -IIc and negatively with bGDGTs -Ia, -Ib and -Ic.

In the IP-bGDGT fraction, axes 1 and 2 explained less than those in the C-bGDGT fraction, suggesting that the environmental and *nirS* gene abundance data explained the bGDGT data less effectively than those in the C-bGDGT fraction (Fig. 4b). Since bGDGTs-IIIa and IIIc weighted too small on either axis 1 or axis 2, these two bacterial lipids were excluded from the analysis of the pattern correlation between the bGDGT distribution and environmental factors and *nirS* gene abundance. The results were similar to those in the C-bGDGT fraction. The bGDGT-Ia, -Ib or -Ic correlated positively with temperature and pH and negatively with ammonium, nitrite, nitrate and *nirS* gene abundance; bGDGTs-IIIb, -IIa, -IIb and -IIc correlated negatively with temperature and pH and positively with ammonium, nitrite, nitrate and *nirS* gene abundance (Fig. 4b).

3.4. Relationship between bGDGT methylation and bacterial 16S rRNA gene sequences

A new methylation index $R_{(III + II)/I}$ (Eq. (3)) was developed based on the RDA analysis (see 3.2) to delineate the relationship between

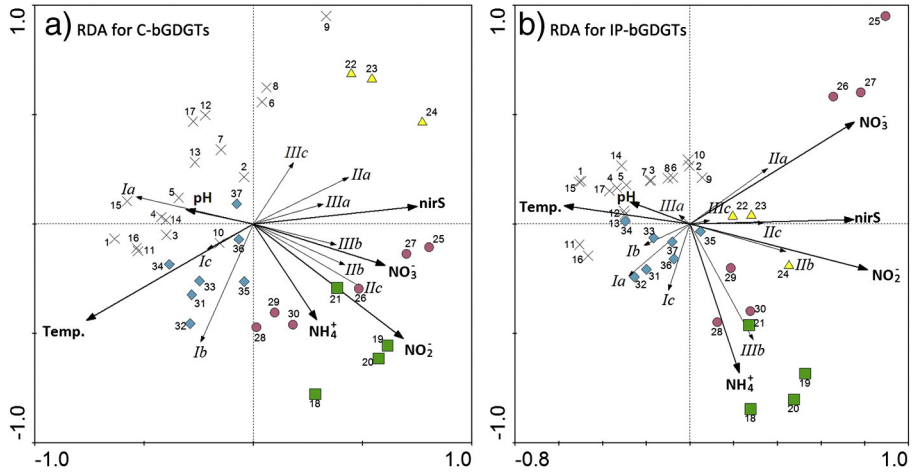

Fig. 4. RDA analysis based on the correlation between the hot spring sediment bGDGT compositions and the distributions of environmental factors and *nirS* gene in the C-bGDGT fraction (a) and the IP-bGDGT fraction (b). The numbers in the plot refer to the hot spring samples in the Table 1. Sample 1 represents GL-4 and sample 37 represents QC-9. Hot spring sediment samples are labeled according to Fig. 3. The horizontal dashed line represents axis 1 on which the variables weight whereas the vertical dashed line represents axis 2. The large vectors represent environmental factors (temperature, pH, ammonium, nitrite and nitrate) and *nirS* gene. The small vectors represent bGDGTs. The Roman numerals refer to structures of bGDGTs in Fig. 1.

bGDGT methylation and the bacterial community phylotypes based on pyrosequencing:

$$R_{(III+II)/I} = [IIIa + IIIb + IIIc + IIa + IIb + IIc]/[Ia + Ib + Ic] \quad (3)$$

where the Roman numerals referred to the bGDGT structures in Fig. 1.

Two bacterial phyla identified in Wang et al. (2013) in the nine hot springs (GL-13-4, GL-20, GL-21, NQ-4, GZ-1, NM-6, NM-7, QC-7 and QC-9) were found to correlate with $R_{(III + II)/I}$ in the C- and IP-bGDGT fractions (Fig. 5). The phyla *Proteobacteria* and *Bacteroidetes* correlated positively with $R_{(III + II)/I}$ in the C-bGDGT fraction (Fig. 5a). In the IP-bGDGT fraction, these correlations were also observed and one of them (correlation between *Bacteroidetes* and $R_{(III + II)/I}$) was stronger than that in the C-bGDGT fraction (Fig. 5b), which is inconsistent with the result of RDA analysis (Fig. 4). This discrepancy may be due to the fact that re-analysis of the pyrosenquencing data was only based on nine hot spring sediment samples rather than all hot spring samples.

In a more detailed analysis, we attempted to determine which of the taxa identified by Wang et al. (2013) at the genus level correlated with $R_{(III + II)/I}$ index or individual bGDGT distribution (Table 2). *Thiobacillus* of the class *Betaproteobacteria* correlated positively with $R_{(III + II)/I}$ in the C- and IP-bGDGTs (Table 2). In the IP-bGDGT fraction, *Thiobacillus* correlated positively with bGDGT-IIc (Table 2). These correlations were better reflected in the IP-bGDGT fraction than in the C-bGDGT fraction. Additionally, in the C-bGDGT fraction, significant positive correlation existed between *Candidatus* Solibacter of the phylum *Acidobacteria* and the distribution of bGDGT-IIc (Suppl. Table 1).

Table 2
Correlations between C-bGDGTs or IP-bGDGTs and the bacterial genera from the reanalyses of pyrosequencing data in nine of the Tibetan hot springs (Wang et al., 2013). Significant correlations are in bold.

Lipids			Genera
			Thiobacillus
C-bGDGTs	bGDGT-IIc	Bivariate correlation	0.019
		Sig. (2-tailed)	0.962
	$R_{III + II/I}$	Bivariate correlation	**0.840**
		Sig. (2-tailed)	**0.005**
IP-bGDGTs	bGDGT-IIa	Bivariate correlation	0.576
		Sig. (2-tailed)	0.105
	bGDGT-IIb	Bivariate correlation	0.632
		Sig. (2-tailed)	0.068
	bGDGT-IIc	Bivariate correlation	**0.699**
		Sig. (2-tailed)	**0.036**
	$R_{III + II/I}$	Bivariate correlation	**0.776**
		Sig. (2-tailed)	**0.014**

4. Discussion

4.1. Factors affecting nitrogen speciation in Tibetan hot springs

Ammonium (NH_4^+) was more abundant than oxidized nitrogen species (nitrite and nitrate) in most springs, which is consistent with nitrogen speciation patterns in other geothermal systems such as Yellowstone National Park (Zhang et al., 2008; Holloway et al., 2011) and the U.S. Great Basin (Dodsworth et al., 2011; Vick et al., 2010). The concentrations of ammonium, nitrite, and nitrate in Tibetan hot springs are also within the range of these species observed in pristine geothermal springs (Holloway et al., 2011; Dodsworth et al., 2011). Sources of ammonium are largely controlled by the sedimentary nature of the subsurface formation and processes affecting the abundance of nitrogen species may be chemical (e.g., pH), physical (e.g., temperature) or biological (e.g., nitrification vs. denitrification) (Holloway et al., 2011; Dodsworth et al., 2011). The wide occurrence of *amoA* gene encoding ammonia-oxidizing archaea (AOA) in terrestrial hot springs (Zhang et al., 2008; Jiang et al., 2010) and the enrichment and isolation of thermophilic AOA (de la Torre et al., 2008; Hatzenpichler et al., 2008) suggest that these organisms may play an important role in controlling the abundance of ammonium in Tibetan hot springs. On the other hand, ammonia-oxidizing bacteria (AOB) appear to play a less important role in the consumption of ammonium in hot springs, particularly when temperature exceeds 50 °C, since few reports exist of thermophilic AOB. The relatively high concentration of nitrite, particularly in Nima hot spring, may indicate that chemolithotrophic oxidation of ammonia supplied in the source water is faster than

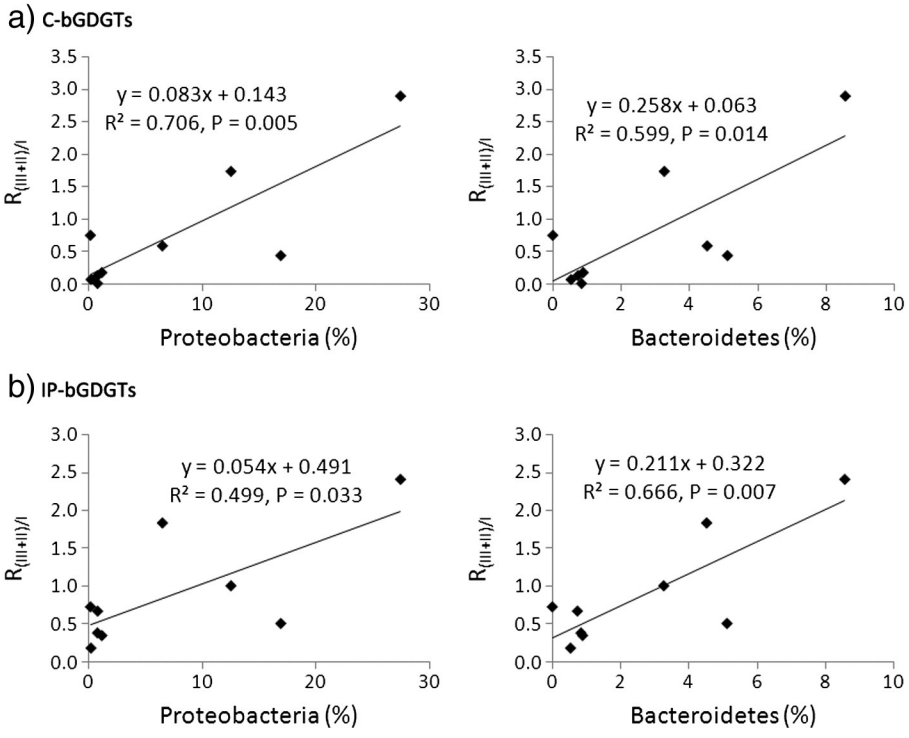

Fig. 5. Linear correlations between $R_{(III + II)/I}$ and bacterial phyla in the C- and IP-bGDGT fractions in nine hot spring sediment samples.

consumption of nitrite, either by assimilation, chemolithotrophic oxidation (nitrification), or anaerobic respiration (denitrification). However, the presence of the *nirS* gene in Tibetan hot springs, as determined by PCR targeting some *Betaproteobacteria* and *Gammaproteobacteria nirS* genes, suggests that bacterial nitrite reduction may occur in these environments, as has been documented in other terrestrial geothermal springs (Dodsworth et al., 2011; Hedlund et al., 2011).

4.2. The origin of bGDGTs detected in Tibetan hot springs

Schouten et al. (2007) were the first to report the presence of bGDGTs in Yellowstone hot springs, which was interpreted to have been mainly introduced by soil runoff. The authors, however, also suggested the possibility of in situ production of bGDGTs in the hot spring environment, which was validated by observations in Great Basin (Hedlund et al., 2013; Zhang et al., 2013) and Tibetan (He et al. 2012) hot springs. Results of the current study further support these observations by showing that the bGDGT abundance is generally much higher in hot springs than in surrounding soils and that significant correlations exist between C- and IP-bGDGTs in hot springs.

4.3. Temperature, pH and nitrogen species effect on bGDGTs in Tibetan hot springs and implications for the biological sources of bGDGTs

Weijers et al. (2007a) found that the calculated MBT index correlated positively with temperature, whereas Peterse et al. (2012) observed that temperature correlated negatively with the relative abundances of bGDGTs-IIIa and -IIa and positively with bGDGT-Ia. These correlations, which were originally based on soil samples, are supported by correlations examined between temperature and bGDGTs in the Tibetan hot springs of this study but not in the previously studied Great Basin (Hedlund et al., 2013; Zhang et al., 2013) or Tibetan (He et al., 2012) hot springs.

In the same soil samples studied by Weijers et al. (2007a) and Peterse et al. (2012), pH was observed to correlate negatively with the calculated CBT index (Weijers et al., 2007a) or bGDGT-Ia (Peterse et al., 2012) and positively with bGDGTs-Ib, -IIb and -IIc (Peterse et al., 2012). The non-metric multidimensional scaling analysis by Hedlund et al. (2013) suggested weak correlations between pH and bGDGTs with less methylated bGDGTs favoring high pH conditions. Our study also showed similar weak correlations between pH and the bGDGT distribution. The inconsistency between hot spring (Hedlund et al., 2013 and this study) and soil environments (Weijers et al., 2007a; Peterse et al., 2012) may be explained by the alkaline range of pH in the hot springs of the Great Basin (6.8 to 10.7) and Tibet (7.0 to 9.1), which is in contrast to the much wider and often acidic pH conditions in soils and peat bogs. Hot springs also are characterized by distinct water chemistry and unique bacterial populations (Zhang et al., 2008; Boyd et al., 2013; Cole et al., 2013; Hou et al., 2013), which may contribute to unique distributions of bGDGTs in the hot springs.

In Tibetan hot springs, multiple environmental factors (e.g. reduced and oxidized fixed nitrogen species) correlated with the distribution of the C- and IP- fractions of bGDGTs. Additionally, these correlations appeared to be stronger in the C-bGDGT fraction than the IP-bGDGT fraction. This suggests that the C-bGDGTs may be more reliable indicators of the interplay between the extant organisms producing bGDGTs and the surrounding environment. One explanation may be that the majority of C-bGDGTs are derived from hydrolysis of the more labile phospholipids that are better indicators for the presence of living cells (Harvey et al., 1986; Schouten et al., 2010; Peterse et al., 2011a) whereas the IP-bGDGTs are mainly derived from more recalcitrant glycolipids that can resist degradation for much longer time and may be preserved on geological scales (Schouten et al., 2010). This is partially supported by our incubation experiment using soil samples that showed persistent presence of IP-bGDGTs at temperatures up to 85 °C for 30 days (unpublished data). Given that the observed core structures of the C-bGDGT fraction were more abundant in their concentration than those of the counterpart IP-bGDGT fraction (Fig. 3a), it is suggested that the bGDGT-producing bacteria in Tibetan hot springs have high regeneration rate (Lipp et al., 2008; Liu et al., 2010), and the amount of glycosidic lipids decorated in such bacterial membrane is small relative to the membrane lipids decorated with phosphate head group (Weijers et al., 2011).

The observed correlations between DIN species and the distribution of bGDGTs suggest that the bGDGT-producing organisms may actively participate in nitrogen metabolism in Tibetan hot springs. The *nirS* gene abundance, as determined by PCR with primers targeting sequences that are conserved in *Beta-* and *Gammaproteobacteria nirS* genes (Li et al., 2013; Throbäck et al., 2004) correlated positively with highly methylated bGDGTs and negatively with minimally methylated bGDGTs. These observations lead us to hypothesize that the genetic capacity for *nirS*-encoded nitrite reduction is a physiological trait of the source organisms synthesizing more bGDGTs with a high degree of methylation (e.g. bGDGTs-IIIa, -IIIb,-IIIc, -IIa, -IIb and -IIc) in Tibetan hot springs. Based on these observations, a new methylation index ($R_{(III + II)/I}$) was proposed to identify some of the potential bGDGT-synthesizing *Proteobacteria* that harbor a *nirS* gene in their genomes.

The relative abundance of the bacterial phylum *Proteobacteria* correlated positively with $R_{(III + II)/I}$. Interestingly, many representatives of the genera *Thiobacillus* and *Pseudomonas* in these two phyla are known to utilize the *nirS* gene product for the reduction of nitrite to nitric oxide (Zumft, 1997; Beller et al., 2006, 2013), which can be subsequently denitrified or ammonified (Simon and Klotz, 2013). Residence of these genera has been verified in nine of the Tibetan hot springs (Wang et al., 2013). In particular, the presence and distribution of the proteobacterial genus *Thiobacillus* correlated positively with $R_{(III + II)/I}$ and the distribution of bGDGT-IIc. The relationship between the phylum *Bacteroidetes* and $R_{(III + II)/I}$, described here, is consistent with the significant correlation between *Bacteroidetes* and the total abundance of C- and IP-bGDGTs in cellulolytic enrichments in a Great Basin hot spring (Zhang et al., 2013). These data suggest that bGDGT-synthesizing bacteria may be affiliated with the two phyla *Proteobacteria* and *Bacteroidetes*.

Acidobacteria are likely biological sources of bGDGTs in peat bogs and soils (Weijers et al., 2006a; Sinninghe Damsté et al., 2011). No significant correlation between *Acidobacteria* and $R_{(III + II)/I}$ was observed in this study. However, *Acidobacteria* correlated positively with the relative abundance of bGDGT-IIc in the IP-bGDGT fraction ($R = 0.790$, $P = 0.011$). Through the genomic analyses, Ward et al. (2009) postulated that the strain Ellin6076 in the genus *Candidatus* Solibacter of the *Acidobacteria* encoded the ability to use cellulose as the carbon source and reduce nitrate/nitrite. In our study, the relative abundance of the genus *Candidatus* Solibacter positively correlated with the relative abundance of bGDGT-IIc in nine of the hot springs, suggesting that "*Candidatus* Solibacter" may be a source of bGDGTs. In contrast, Zhang et al. (2013) did not find any significant correlation between *Acidobacteria* and bGDGTs in a Great Basin hot spring, suggesting that some organisms producing bGDGTs in the hot springs may be different from those in the soil environment.

5. Summary and conclusions

Through the analyses of absolute and relative concentrations of C-bGDGTs and IP-bGDGTs, we revealed that hot spring bGDGTs are predominantly formed in situ. The RDA analyses suggest that concentrations of ammonium, nitrite, nitrate and log transformation values of proteobacterial *nirS* gene abundance correlated positively with the distribution of bGDGTs-IIIa, -IIIb, -IIIc, -IIa, -IIb and -IIc and negatively with the distribution of bGDGTs-Ia, -Ib and -Ic, which can be defined by a new methylation index ($R_{(III + II)/I}$). Through reanalysis of published bacterial 16S rRNA gene pyrotags from nine of the Tibetan hot springs, the phyla *Proteobacteria* and *Bacteroidetes* were positively

correlated with the new index $R_{(III + II)/I}$ and some representatives of these *Proteobacteria* (including *Thiobacillus*, which positively correlated with $R_{(III + II)/I}$) encode the *nirS* gene in their genomes. Our results suggest that some of the thermotolerant or thermophilic bacteria with the genetic potential of *nirS*-encoded nitrite reduction and/or members of the *Bacteroidetes* may be the biological sources of heavily methylated bGDGTs in Tibetan hot springs. Despite these observations, to our knowledge, none of the thermophilic organisms mentioned above have been tested for the production of bGDGTs in pure cultures. To test our hypothesis, future studies will focus on studying moderately thermophilic or thermotolerant *Proteobacteria* and *Bacteroidetes* for their capacity to synthesize methylated bGDGTs.

Supplementary data to this article can be found online at http://dx.doi.org/10.1016/j.chemgeo.2014.08.015.

Acknowledgments

We thank Yong Zhang, Zhaoqi Song and Huilei Ren for sampling hot spring sediments and surrounding soils and measuring environmental parameters in the field, Liang Dong and Jinxiang Wang for assistance in the laboratory experiments, and Huanye Wang and Wei Xie for analytical assistance. The constructive comments from two anonymous reviewers significantly improved the quality of a previous version of the manuscript. This study was funded by the National Natural Science Foundation of China grants # 40972211 and #4137372, the US National Science Foundation grants # ETBC-1024614 and #OISE-0968421, the Key Projects of International Cooperation of Ministry of Science & Technology (MOST) of China (2013DFA31980), and the "Thousand Talents Program" (91028005) and the State Key Laboratory of Marine Geology at Tongji University (4137372). MGK was supported by the Visiting Scholar Funds of Tongji University (TJ2012-017) and the Research Incentive Funds from the University of North Carolina at Charlotte (675612).

References

Ballantyne, A.P., Greenwood, D.R., Sinninghe Damsté, J.S., Csank, A.Z., Eberle, J.J., Rybczynski, N., 2010. Significantly warmer Arctic surface temperatures during the Pliocene indicated by multiple independent proxies. Geology 38, 603–606.

Beller, H.R., Chain, P.S., Letain, T.E., Chakicherla, A., Larimer, F.W., Richardson, P.M., et al., 2006. The genome sequence of the obligately chemolithoautotrophic, facultatively anaerobic bacterium *Thiobacillus denitrificans*. J. Bacteriol. 188, 1473–1488.

Beller, H.R., Zhou, P., Legler, T.C., Chakicherla, A., Kane, S., Letain, T.E., O'Day, P.A., 2013. Genome-enabled studies of anaerobic, nitrate-dependent iron oxidation in the chemolithoautotrophic bacterium *Thiobacillus denitrificans*. Front. Microbiol. 4, 222.

Bendle, J.A., Weijers, J.W.H., Maslin, M.A., Sinninghe Damsté, J.S., Schouten, S., Hopmans, E. C., et al., 2010. Major changes in glacial and Holocene terrestrial temperatures and sources of organic carbon recorded in the Amazon fan by tetraether lipids. Geochem. Geophys. Geosyst. 11, Q12007.

Blaga, C.I., Reichart, G.J., Heiri, O., Sinninghe Damsté, J.S., 2009. Tetraether membrane lipid distributions in water-column particulate matter and sediments: a study of 47 European lakes along a north-south transect. J. Paleolimnol. 41, 523–540.

Boyd, E.S., Hamilton, T.L., Wang, J., He, L., Zhang, C.L., 2013. The role of tetraether lipid composition in the adaptation of thermophilic archaea to acidity. Front. Microbiol. http://dx.doi.org/10.3389/fmicb.2013.00062.

Cole, J.K., Peacock, J.P., Dodsworth, J.A., Williams, A.J., Thompson, D.B., Dong, H., et al., 2013. Sediment microbial communities in Great Boiling Spring are controlled by temperature and distinct from water communities. ISME J. 7, 718–729.

de La Torre, J.R., Walker, C.B., Ingalls, A.E., Könneke, M., Stahl, D.A., 2008. Cultivation of a thermophilic ammonia oxidizing archaeon synthesizing crenarchaeol. Environ. Microbiol. 10, 810–818.

Dodsworth, J.A., Hungate, B.A., Hedlund, B.P., 2011. Ammonia oxidation, denitrification and dissimilatory nitrate reduction to ammonium in two US Great Basin hot springs with abundant ammonia-oxidizing archaea. Environ. Microbiol. 13, 2371–2386.

Fawcett, P.J., Werne, J.P., Anderson, R.S., Heikoop, J.M., Brown, E.T., Berke, M.A., et al., 2011. Extended megadroughts in the southwestern United States during Pleistocene interglacials. Nature 470, 518–521.

Harvey, H.R., Fallon, R.D., Patton, J.S., 1986. The effect of organic matter and oxygen on the degradation of bacterial membrane lipids in marine sediments. Geochim. Cosmochim. Acta 50, 795–804.

Hatzenpichler, R., Lebedeva, E.V., Spieck, E., Stoecker, K., Richter, A., Daims, H., Wagner, M., 2008. A moderately thermophilic ammonia-oxidizing crenarchaeota from a hot spring. Proc. Natl. Acad. Sci. U. S. A. 105, 2134–2139.

He, L., Zhang, C.L., Dong, H., Fang, B., Wang, G., 2012. Distribution of glycerol dialkyl glycerol tetraethers in Tibetan hot springs. Geosci. Front. 3, 289–300.

Hedlund, B.P., Mcdonald, A.I., Lam, J., Dodsworth, J.A., Brown, J.R., Hungate, B.A., 2011. Potential role of *Thermus thermophilus* and *T. oshimai* in high rates of nitrous oxide (N_2O) production in ~80 °C hot springs in the US Great Basin. Geobiology 9, 471–480.

Hedlund, B.P., Paraiso, J.J., Williams, M.J., Huang, Q., Wei, Y., Dijkstra, P., et al., 2013. Wide distribution of autochthonous branched glycerol dialkyl glycerol tetraethers (bGDGTs) in U.S. Great Basin hot springs. Front. Microbiol. 4, 222.

Holloway, J.M., Nordstrom, D.K., Böhlke, J.K., McCleskey, R.B., Ball, J.W., 2011. Ammonium in thermal waters of Yellowstone National Park: processes affecting speciation and isotope fractionation. Geochim. Cosmochim. Acta 75, 4611–4636.

Hopmans, E.C., Weijers, J.W.H., Schefuss, E., Herfort, L., Sinninghe Damsté, J.S., Schouten, S., 2004. A novel proxy for terrestrial organic matter in sediments based on branched and isoprenoid tetraether lipids. Earth Planet. Sci. Lett. 224, 107–116.

Hou, W., Wang, S., Dong, H., Jiang, H., Briggs, B.R., Peacock, J.P., et al., 2013. A comprehensive census of microbial diversity in hot spring of Tengchong, Yunnan Province China using 16S rRNA gene pyrosequencing. PLoS ONE 8, e53350.

Jiang, H., Huang, Q., Dong, H., Wang, P., Wang, F., Li, W., Zhang, C., 2010. RNA-based investigation of ammonia-oxidizing archaea in hot springs of Yunnan Province, China. Appl. Environ. Microbiol. 76, 4538–4541.

Lepš, Jan, PetrŠmilauer, 2003. Multivariate Analysis of Ecological Data using CANOCO. Published in the United States of America by Cambridge University Press, New York.

Li, F., Zhang, C.L., Dong, H., Li, W., Williams, A., 2013. Environmental controls on the distribution of archaeal lipids in Tibetan hot springs: insight into the application of organic proxies for biogeochemical processes. Environ. Microbiol. Rep. 5, 868–882.

Lipp, J.S., Morono, Y., Inagaki, F., Hinrichs, K.U., 2008. Significant contribution of Archaea to extant biomass in marine subsurface sediments. Nature 454, 991–994.

Liu, X.L., Leider, A., Gillespie, A., Gröger, J., Versteegh, G.J.M., Hinrichs, K.U., 2010. Identification of polar lipid precursors of the ubiquitous branched GDGT orphan lipids in a peat bog in Northern Germany. Org. Geochem. 41, 653–660.

Peterse, F., Schouten, S., van der Meer, J., van der Meer, M.T.J., Sinninghe Damsté, J.S., 2009a. Distribution of branched tetraether lipids in geothermally heated soils: implications for the MBT/CBT temperature proxy. Org. Geochem. 40, 201–205.

Peterse, F., Kim, J.H., Schouten, S., Kristensen, D.K., Koç, N., Sinninghe Damsté, J.S., 2009b. Constraints on the application of the MBT-CBT paleothermometer at high latitude environments (Svalbard, Norway). Org. Geochem. 40, 692–699.

Peterse, F., Nicol, G.W., Schouten, S., Sinninghe Damsté, J.S., 2010. Influence of soil pH on the abundance and distribution of core and intact polar lipid-derived branched GDGTs in soil. Org. Geochem. 41, 1171–1175.

Peterse, F., Hopmans, E.C., Schouten, S., Mets, A., Rijpstra, W.I.C., Sinninghe Damsté, J.S., 2011a. Identification and distribution of intact polar branched tetraether lipids in peat and soils. Org. Geochem. 42, 1007–1015.

Peterse, F., Prins, M.A., Beets, C.J., Troelstra, S.R., Zheng, H., Gu, Z., et al., 2011b. Decoupled warming and monsoon precipitation in East Asia over the last deglaciation. Earth Planet. Sci. Lett. 301, 256–264.

Peterse, F., van der Meer, J., Schouten, S., Weijers, W.H., Fierer, N., Jackson, R.B., et al., 2012. Revised calibration of the MBT–CBT paleotemperatureproxy based on branched tetraether membrane lipidsin surface soils. Geochim. Cosmochim. Acta 96, 215–229.

Powers, L.A., Werne, J.P., Johnson, T.C., Hopmans, E.C., Sinninghe Damsté, J.S., Schouten, S., 2004. Crenarchaeotal membrane lipids in lake sediments: a new paleotemperature proxy for continental paleoclimate reconstruction? Geology 32, 613–616.

Rueda, G., Rosell-Melé, A., Escala, M., Gyllencreutz, R., Backman, J., 2009. Comparison of instrumental and GDGT-based estimates of sea surface and air temperatures from the Skagerrak. Org. Geochem. 40, 287–291.

Schouten, S., Hopmans, E.C., Pancost, R.D., Sinninghe Damsté, J.S., 2000. Widespread occurrence of structurally diverse tetraether membrane lipids: evidence for the ubiquitous presence of low-temperature relatives of hyperthermophiles. Proc. Natl. Acad. Sci. U. S. A. 97, 14421–14426.

Schouten, S., van der Meer, M.T.J., Hopmans, E.C., Rijpstra, W.I.C., Reysenbach, A.L., Ward, D.M., Sinninghe Damsté, J.S., 2007. Archaeal and bacterial glycerol dialkyl glycerol tetraether lipids in hot springs of Yellowstone National Park. Appl. Environ. Microbiol. 73, 6181–6191.

Schouten, S., Eldrett, J., Greenwood, D.R., Harding, I., Baas, M., Sinninghe Damsté, J.S., 2008. Onset of long-term cooling of Greenland near the Eocene–Oligocene boundary as revealed by branched tetraether lipids. Geology 36, 147–150.

Schouten, S., Middelburg, J.J., Hopmans, E.C., Sinninghe Damsté, J.S., 2010. Fossilization and degradation of intact polar lipids in deep subsurface sediments: a theoretical approach. Geochim. Cosmochim. Acta 74, 2433–2440.

Simon, J., Klotz, M.G., 2013. Diversity and evolution of bioenergetic systems involved in microbial nitrogen compound transformations. Bioch. Biophys. Acta 1827, 114–132.

Sinninghe Damsté, J.S., Hopmans, E.C., Pancost, R.D., Schouten, S., Geenevasen, J.A.J., 2000. Newly discovered non-isoprenoid glycerol dialkyl glycerol tetraether lipids in sediments. Chem. Commun. 2000, 1683–1684.

Sinninghe Damsté, J.S., Ossebaar, J., Abbas, B., Schouten, S., Verschuren, D., 2009. Fluxes and distribution of tetraether lipids in an equatorial African lake: constraints on the application of the TEX_{86} palaeothermometer and BIT index in lacustrine settings. Geochim. Cosmochim. Acta 73, 4232–4249.

Sinninghe Damsté, J.S., Rijpstra, W.I.C., Hopmans, E.C., Weijers, W.H., Foesel, B.U., Overmann, J., Dedysh, S.N., 2011. 13,16-Dimethyl octacosanedioic acid (*iso*-diabolic acid), a common membrane-spanning lipid of *Acidobacteria* subdivisions 1 and 3. Appl. Environ. Microbiol. 77, 4147–4154.

Sun, Q., Chu, G., Liu, M., Xie, M., Li, S., Ling, Y., et al., 2011. Distributions and temperature dependence of branched glycerol dialkyl glycerol tetraethers in recent lacustrine sediments from China and Nepal. J. Geophys. Res. 116, G01008.

Throbäck, I.N., Enwall, K., Jarvis, A., Hallin, S., 2004. Reassessing PCR primers targeting *nirS*, *nirK* and *nosZ* genes for community surveys of denitrifying bacteria with DGGE. FEMS Microbiol. Ecol. 49, 401–417.

Tierney, J.E., Russell, J.M., 2009. Distributions of branched GDGTs in a tropical lake system: implications for lacustrine application of the MBT/CBT paleoproxy. Org. Geochem. 40, 1032–1036.

Tierney, J.E., Schouten, S., Pitcher, A., Hopmans, E.C., Sinninghe Damsté, J.S., 2011. Core and intact polar glycerol dialkyl glycerol tetraethers (GDGTs) in Sand Pond, Warwick, Rhode Island (USA): insights into the origin of lacustrine GDGTs. Geochim. Cosmochim. Acta http://dx.doi.org/10.1016/j.gca.2011.10.018.

Tyler, J.J., Nederbragt, A.J., Jones, V.J., Thurow, J.W., 2010. Assessing past temperature and soil pH estimates from bacterial tetraether membrane lipids: evidence from the recent lake sediments of Lochnagar, Scotland. J. Geophys. Res. 115, G01015.

Vick, T.J., Dodsworth, J.A., Costa, K.C., Shock, E.L., Hedlund, B.P., 2010. Microbiology and geochemistry of little hot creek, a hot spring environment in the Long Valley Caldera. Geobiology 8, 140–154.

Wächtershäuser, G., 2003. From pre-cells to Eukarya—a tale of two lipids. Mol. Microbiol. 47, 13–22.

Wang, H., Liu, W., Zhang, C.L., Wang, Z., Wang, J., Liu, Z., Dong, H., 2012. Distribution of glycerol dialkyl glycerol tetraethers in surface sediments of Lake Qinghai and surrounding soil. Org. Geochem. 47, 78–87.

Wang, S., Hou, W., Dong, H., Jiang, H., Huang, L., Wu, G., et al., 2013. Control of temperature on microbial community structure in hot springs of the Tibetan Plateau. (2013). PLoS ONE 8, e62901.

Ward, N.L., Challacombe, J.F., Janssen, P.H., Henrissat, B., Coutinho, P.M., Wu, M., et al., 2009. Three genomes from the phylum *Acidobacteria* provide insight into the lifestyles of these microorganisms in soils. Appl. Environ. Microbiol. 75, 2046–2056.

Weijers, J.W.H., Schouten, S., Hopmans, E.C., Geenevasen, J.A.J., David, O.R.P., Coleman, J.M., et al., 2006a. Membrane lipids of mesophilic anaerobic bacteria thriving in peats have typical archaeal traits. Environ. Microbiol. 8, 648–657.

Weijers, J.W.H., Schouten, S., Spaargaren, O.C., Sinninghe Damsté, J.S., 2006b. Occurrence and distribution of tetraether membrane lipids in soils: implications for the use of the TEX_{86} proxy and the BIT index. Org. Geochem. 37, 1680–1693.

Weijers, J.W.H., Schouten, S., van den Donker, J.C., Hopmans, E.C., Sinninghe Damsté, J.S., 2007a. Environmental controls on bacterial tetraether membrane lipid distribution in soils. Geochim. Cosmochim. Acta 71, 703–713.

Weijers, J.W.H., Schefuβ, E., Schouten, S., Sinninghe Damsté, J.S., 2007b. Coupled thermal and hydrological evolution of tropical Africa over the last deglaciation. Science 315, 1701–1704.

Weijers, J.W.H., Schouten, S., Sluijs, A., Brinkhuis, H., Sinninghe Damsté, J.S., 2007c. Warm Arctic continents during the Palaeocene–Eocene thermal maximum. Earth Planet Sci. Lett. 261, 230–238.

Weijers, J.W.H., Panoto, E., Van Bleijswijk, J., Schouten, S., Rijpstra, W.I.C., Balk, M., et al., 2009. Constraints on the biological source(s) of the orphan branched tetraether membrane lipids. Geomicrobiol J. 26, 402–414.

Weijers, J.W.H., Wiesenberg, G.L.B., Bol, R., Hopmans, E.C., Pancost, R.D., 2010. Carbon isotopic composition of branched tetraether membrane lipids in soils suggest a rapid turnover and a heterotrophic life style of their source organism(s). Biogeosci. Discuss. 7, 3691–3734.

Weijers, J.W.H., Bernhardt, B., Peterse, F., Werne, J.P., Dungait, J.A.J., Schouten, S., Sinninghe Damsté, J.S., 2011. Absence of seasonal patterns in MBT-CBT indices in mid-latitude soils. Geochim. Cosmochim. Acta 75, 3179–3190.

White, D.C., Davis, W.M., Nickels, J.S., King, J.D., Bobbie, R.J., 1977. Determination of the sedimentary microbial biomass by extractable lipid phosphate. Oecologia 40, 51–62.

Zhang, C.L., Ye, Q., Huang, Z., Li, W., Chen, J., Song, Z., et al., 2008. Global occurrence of Archaeal amoA genes in terrestrial hot springs. Appl. Environ. Microbiol. 74, 6417–6426.

Zhang, C.L., Wang, J., Wei, Y., Zhu, C., Huang, L., Dong, H., 2012. Production of branched tetraether lipids in the lower Pearl River and estuary: effects of extraction methods and impact on bGDGT proxies. Front. Microbiol. http://dx.doi.org/10.3389/fmicb.2011.00274.

Zhang, C.L., Wang, J., Dodsworth, J.A., Williams, A.J., Zhu, C., Hinrichs, K.U., et al., 2013. In situ production of branched glycerol dialkyl glycerol tetraethers in a great basin hot spring (USA). Front Microbiol http://dx.doi.org/10.3389/fmicb.2013.00181.

Zhou, H., Hu, J., Ming, L., Peng, P., Zhang, G., 2011. Branched glycerol dialkyl glycerol tetraethers and paleoenvironmental reconstruction in Zoigê peat sediments during the last 150 years. Chin. Sci. Bull. 56, 2456–2463.

Zhu, C., Weijers, J.W.H., Wagner, T., Pan, J.M., Chen, J.F., Pancost, R.D., 2011. Sources and distributions of tetraether lipids in surface sediments across a large river-dominated continental margin. Org. Geochem. 42, 376–386.

Zink, K.G., Vandergoes, M.J., Mangelsdorf, K., Dieffenbacher-Krall, A.C., Schwark, L., 2010. Application of bacterial glycerol dialkyl glycerol tetraethers (GDGTs) to develop modern and past temperature estimates from New Zealand lakes. Org. Geochem. 41, 1060–1066.

Zumft, W.G., 1997. Cell biology and molecular basis of denitrification. Microbiol. Mol. Biol. Rev. 61, 533.